



## Short communication

# Lithium–sulfur batteries: Influence of C-rate, amount of electrolyte and sulfur loading on cycle performance



Jan Brückner <sup>a</sup>, Sören Thieme <sup>a</sup>, Hannah Tamara Grossmann <sup>a</sup>, Susanne Dörfler <sup>a,b</sup>,  
Holger Althues <sup>a</sup>, Stefan Kaskel <sup>a,b,\*</sup>

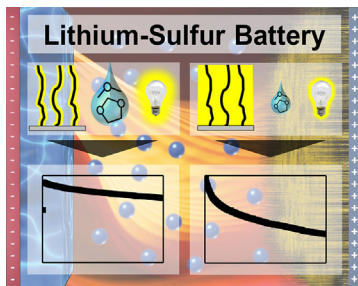
<sup>a</sup> Fraunhofer Institute for Material and Beam Technology (IWS), Winterbergstraße 28, D-01277 Dresden, Germany

<sup>b</sup> Department of Inorganic Chemistry, Dresden University of Technology, Bergstraße 66, D-01062 Dresden, Germany

## HIGHLIGHTS

- Performance of sulfur cathodes depends heavily on amount of electrolyte and C-rate.
- Excess of electrolyte, high rate and low loading lead to seemingly superior results.
- Recently published data regarding new materials should be carefully interpreted.
- Publications on lithium sulfur batteries, need to state the amount of electrolyte.
- Layer transfer of VA-CNT enables light-weight and good mechanical adhesion.

## GRAPHICAL ABSTRACT



## ARTICLE INFO

### Article history:

Received 26 March 2014

Received in revised form

12 May 2014

Accepted 29 May 2014

Available online 12 June 2014

### Keywords:

Lithium sulfur battery

Electrochemistry

Sulfur loading

Electrolyte

Degradation

## ABSTRACT

In the past four years major improvement of the lithium sulfur battery technology has been reported. Novel carbon cathode materials offer high sulfur loading, sulfur utilization and cycle stability. An often neglected aspect is that sulfur loading and amount of electrolyte strongly impact the performance. In this paper, we demonstrate how the amount of electrolyte, sulfur loading, lithium excess and cycling rate influences the cycle stability and sulfur utilization. We chose vertically aligned carbon nanotubes (VA-CNT) as model system with a constant areal loading of carbon. For a high reproducibility, decreased weight of current collector and good mechanical adhesion of the VA-CNTs we present a layer transfer technique that enables a light-weight sulfur cathode. The sulfur loading of the cathode was adjusted from 20 to 80 wt.-%. Keeping the total amount of electrolyte constant and varying the C-rate, we are able to demonstrate that the capacity degradation is reduced for high rates, high amount of electrolyte and low sulfur loading. In addition idle periods in the cycling regimen and lower rates result in an increased degradation. We attribute this to the redox-reaction between reactive lithium and polysulfides that correlates with the cycling time, rather than cycle number.

© 2014 Elsevier B.V. All rights reserved.

## 1. Introduction

The lithium sulfur battery system is investigated as a post-lithium-ion technology, promising high gravimetric energy

\* Corresponding author. Department of Inorganic Chemistry, Dresden University of Technology, Bergstraße 66, D-01062 Dresden, Germany. Tel.: +49 35146333632.

E-mail address: [stefan.kaskel@chemie.tu-dresden.de](mailto:stefan.kaskel@chemie.tu-dresden.de) (S. Kaskel).

densities and decreased material costs due to the cheap, abundant and non-toxic sulfur. Although the underlying cell chemistry and – at least in principle – reversible electrochemical reactions were already known and investigated in the late 1970s [1,2], the field was invigorated by Nazar and co-worker in 2009 [3]. Using a mesoporous carbon material and a polymer-coating, it was shown that the sulfur utilization could be as high as 1300 mAh g<sup>-1</sup> sulfur and polysulfide dissolution could be hindered. Many more advanced carbon structures were presented in the following years that allowed for an improvement in both the sulfur content of the composite as well as the areal [4–9]. Recently, papers were published showing 1000 and more cycles [8,10–15].

In the past two years, the measurement conditions were standardized to some extent. It is now understood that lithium nitrate hinders the shuttle mechanism by forming a more stable SEI on the surface of the metallic lithium anode [16,17]. Further, Zhang showed that lithium nitrate is irreversibly reduced below 1.6 V [18]. This is especially noteworthy since cycling conditions (voltage window) should be adjusted, otherwise initial capacities may be largely overestimated. Even more severely: when a cell setup employs a large excess of electrolyte, the depletion of lithium nitrate is usually not recognized due to the high LiNO<sub>3</sub>-to-S ratio. As a result, the irreversible capacity of its decomposition is attributed to reversible cycling of sulfur species [12,13,19,20].

Recently, the so-called “concept of the two lows” was introduced [21,22]. The authors point out that low sulfur content in the cathode and a low areal loading is not suitable for a practical application.

Finally, there has been a recent publication looking more closely on the amount of electrolyte that is needed to achieve reversible cycling [23]. Besides the minimal electrolyte-to-sulfur ratio, we also demonstrated that a limited amount of electrolyte leads to cell failure due to the cell running dry, which is caused by the instability of the solvent molecules versus metallic lithium [8]. This degradation mechanism is accelerated at high areal currents [24] and a low excess of lithium [25] as dendrite formation is more pronounced under these conditions.

In this paper, we demonstrate the necessity of clearly stating the amount of electrolyte, lithium excess, sulfur content and areal loading used in the test setup to compare published results. For this purpose, we chose aluminum based VA-CNT film as a model system with an almost ideal open and accessible pore structure between the individual, electrically contacted nanotubes. Since many publications aim to encapsulate the sulfur and claim that this is needed to achieve reversible and stable cycling, this open pore structure is supposed to be counterproductive. We show how the amount of electrolyte and areal sulfur loading significantly influences the rate capability, cycle stability and can lead to a new interpretation of present results.

## 2. Experimental

### 2.1. VA-CNT synthesis

The detailed catalyst coating procedure and subsequent CVD process for the preparation of vertically aligned carbon nanotube (VA-CNT) electrodes is described elsewhere [5]. The VA-CNTs were grown on a nickel foil (50 µm, Ra = 25 nm) (Alfa Aesar, 99% Ni), which was cut into 3.5 × 6 cm<sup>2</sup> pieces and dip-coated with an alumina-precursor. Afterward, the foil was dip-coated with the catalyst precursor, which was a 0.22 m solution of Fe(2-ethylhexanoate)<sub>3</sub> (Alfa Aesar, 50% in mineral spirits) and Co(2-ethylhexanoate)<sub>2</sub> (Sigma Aldrich, 65% in mineral spirits) in 2-propanol (Carl Roth, >99.8%). The VA-CNT films were grown at atmospheric pressure in a quartz tube reactor (40 mm diameter) for

20 min at 730 °C and 1 standard liter per minute (slm) argon, 0.7 slm hydrogen, 0.18 slm ethene and 0.01 slm argon (water bubbler). The areal loading was 1 (±0.1) mgVA-CNT cm<sup>-2</sup>.

### 2.2. Layer transfer

Using a hot press (Labopress P 200T, Vogt Maschinenbau GmbH) the VA-CNT layer was transferred to a primer-coated (5 µm) 15 µm aluminum foil (Pi-Kem) at 80 °C and 15 bar system pressure, at a typical sample size of 3.5 × 6 cm<sup>2</sup>. The VA-CNTs are pressed into the softened primer. After 5 min the press is cooled below 30 °C and the VA-CNTs can easily be peeled off the nickel foil.

### 2.3. Electrode preparation

Sulfur was melt infiltrated in the layer-transferred VA-CNT electrodes at 155 °C under lab atmosphere. Due to the hydrophobic nature of both VA-CNTs and sulfur, in combination with the open pore structure, the infiltration was completed within seconds of reaching the melting point of sulfur. The high mechanical stability of the layer transferred VA-CNTs enabled uniform sulfur casting before infiltration. The sulfur loading was calculated from the weight increase and was 21.4, 41.0, 60.9 and 80.4 wt.-% for the samples S20, S40, S60 and S80, respectively. Using this method of preparing a sulfur/carbon composite, the weight can only be controlled to approximately 1 wt.-%. Circular electrodes with a diameter of 12 mm (21.4, 41.0 and 80.4 wt.-% sulfur loading) and 10 mm (60.9 wt.-% sulfur loading) were punched from the electrode sheets.

### 2.4. Electrochemical testing

Coin cells (MTI Corp., CR2016) were assembled in an Argon-filled glove box (MBraun, <0.1 ppm O<sub>2</sub> and H<sub>2</sub>O). As anode material, metallic lithium (Pi-Kem, 99.0%, diameter 15.6 mm, thickness 250 µm) was used. The electrodes were separated by one layer of a polypropylene separator (Celgard 2500). The electrolyte consisted of 1 M lithium bis(trifluoromethylsulfonyl) imide (LiTFSI, Aldrich, 99.95%), 0.25 m lithium nitrate (LiNO<sub>3</sub>, Alfa Aesar, 99.98%, anhydrous) in 1,2-dimethoxy ethane (DME, Sigma Aldrich, 99.5%, anhydrous) and 1,3-dioxolane (DOL, Sigma Aldrich, 99.8%, anhydrous). The ratio of the solvents was 1:1 (v/v). The cells were cycled at room temperature with a BaSyTec Cell Test System (CTS). The lower and upper cut-off voltage was 1.8 and 2.6 V, respectively. The amount of electrolyte, added to all coin cells, was constant at 20 µL. All chemicals except for LiTFSI, DME, and DOL were used as received. To remove residual water, LiTFSI was dried at 120 °C under vacuum for 24 h before use. DME and DOL were dried and stored over a 3 E molecular sieve.

### 2.5. VA-CNT morphology characterization

SEM images were acquired with a JEOL JSM-6610LV scanning electron microscope.

## 3. Results and discussion

### 3.1. Layer transfer

Electrodes based on VA-CNTs are good model systems [5,26]. Due to the point contact of the VA-CNTs to the substrate the conductivity is very high and suitable for high power applications such as supercapacitors [27]. Our group was able to translate the results from Hata et al. [28] to a CVD process that uses buffer and precursor solutions which can be wet-chemically applied. However, as

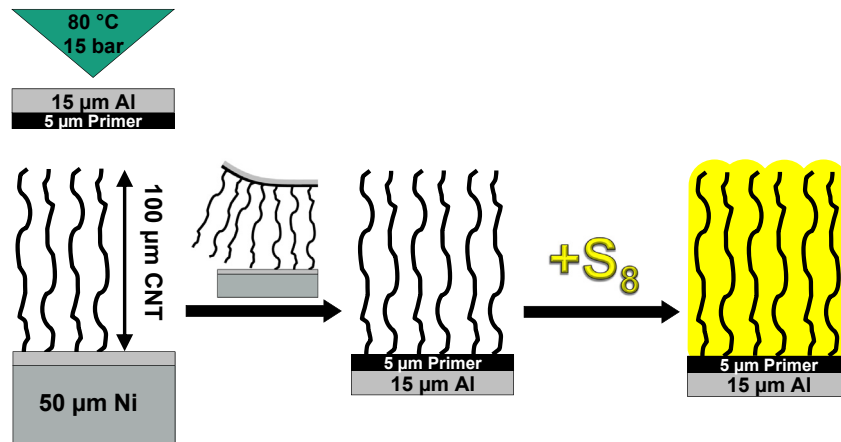


**Fig. 1.** Scheme of two-step layer transfer process. Firstly the VA-CNTs are transferred from nickel substrate to primer-coated, battery-grade aluminum foil. The VA-CNTs exhibit a much higher mechanical stability and sulfur can easily be casted for melt infiltration.

optimal CNT-growth is obtained at 730 °C, nickel with a minimal thickness of 50 μm is needed as the substrate rather than a desirable thin aluminum foil ( $T_m = 660$  °C). Consequently, the weight ratio of nickel to VA-CNTs is approximately 43:1 for a single-side coating of 1 mg cm<sup>-2</sup> VA-CNT corresponding to a height of approx. 100 μm of the VA-CNT film. Further, the VA-CNTs exhibit a very low adhesion to the substrate, despite their point contact, and are easily delaminated when shearing forces are applied. In contrast, the VA-CNTs are not compressed upon applying vertical pressure due to their out-standing mechanical properties and strong van-der-Waals interactions.

Based on these properties, we developed a simple layer transfer technique in which the VA-CNTs can be transferred to a 15 μm

thick, primer-coated, battery grade aluminum foil (Fig. 1). At a temperature of 80 °C the primer is softened and the VA-CNTs are pressed into the primer with a well-defined pressure. Once the temperature is lowered again the VA-CNTs can easily be peeled off the nickel foil. A simple peel test demonstrates the good adhesion of the VA-CNTs to the substrate (Fig. 2a). Scratch tests confirmed that the primer delaminates, and with it, the incorporated VA-CNTs can be removed (Fig. 2b). SEM analysis verified that the CNTs are still vertically aligned after layer transfer (S1). For the presented samples the weight of the current collector is reduced by 90% to 5 mg cm<sup>-2</sup>. In addition, we were able to reproduce these results using a 12 μm aluminum foil with a 1 μm primer coating. This setup reduces the weight by additional 32% to 3.4 mg cm<sup>-2</sup> entire

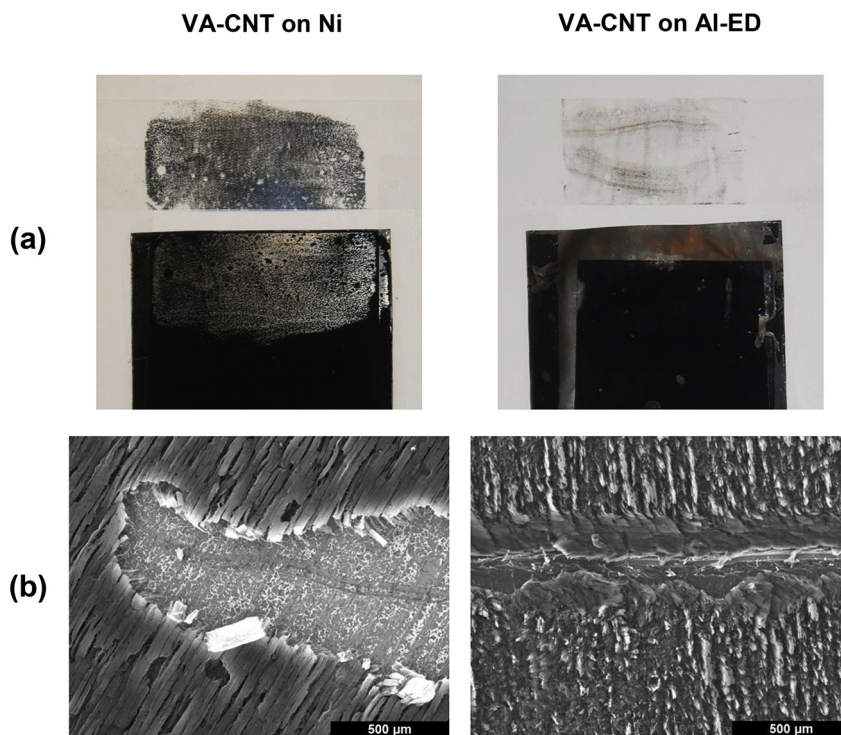


**Fig. 2.** (a) Peel test: almost all VA-CNTs adhere to the tape for nickel substrate, whereas minimal loss is observed for VA-CNTs impressed and transferred to the primer-coated aluminum substrate. (b) Scalpel scratch test: SEM images clearly demonstrate the higher adhesion for VA-CNTs on primer-coated aluminum foil. For the transferred sample the VA-CNTs are knocked over rather than detached.

**Table 1**  
Sample data.

Sample-	Sulfur loading	Electrolyte		Current		Lithium excess
	wt.-% $\text{mg}_{\text{sulfur}} \text{cm}^{-2}$	$\mu\text{l}$	$\mu\text{l mg}^{-1}$ sulfur	C-rate	$\text{mA cm}^{-2}$	$\% \text{Li cm}^{-2}$
S20-C5	21.4	0.23	20	78.5	0.2	0.08
S40-C5	41.0	0.80	20	22.2	0.2	0.27
S60-C5	60.9	1.47	20	17.4	0.2	0.49
S80-C5	80.4	4.87	20	3.6	0.2	1.63
S20-1 mA	21.4	0.24	20	72.4	2.5	1.00
S40-1 mA	41.0	0.75	20	23.7	0.8	1.00
S60-1 mA	60.9	1.46	20	17.5	0.4	1.00
S80-1 mA	80.4	4.76	20	3.7	0.1	1.00
						507

electrode weight. Due to the higher mechanical adhesion, uniform sulfur distribution for melt infiltration is much easier ensured.

### 3.2. Electrochemical testing and theoretical aspects

With a constant VA-CNT loading of  $1 \text{ mg}_{\text{VA-CNT}} \text{ cm}^{-2}$ , sulfur was added to achieve 20, 40, 60 and 80 wt.-% in the cathode. This results in sulfur loadings ranging from very low 0.2 to high  $4.8 \text{ mg}_{\text{sulfur}} \text{ cm}^{-2}$ . Because of the unique structure, no binder or conductive additive is needed in VA-CNT electrodes. Electrochemical tests were conducted using a constant amount of electrolyte of  $20 \mu\text{l}$ , which is the minimal amount for our coin cell setup. Consequently, the relative amount of electrolyte varies from 79 down to  $4 \mu\text{l mg}_{\text{sulfur}}^{-1}$  (Table 1). Moreover, all sulfur loadings were tested using a constant C-rate of C/5 ("C5" samples) or a constant current density of  $1 \text{ mA cm}^{-2}$  ("1 mA" samples). Due to the constant carbon loading, the actual current for S80-C5 is twice as high as for S80-1 mA whereas it is only 10% for S20-C5 of the S20-1 mA current. This is especially noteworthy as reported high rate capabilities should often rather be attributed to the low areal loading and electrolyte excess than the carbon structure. These parameters are comparable to a "catholyte system" [11] with its major drawback of low energy density. We also calculated the lithium excess for the different cells. The data is summarized in Table 1.

One should keep in mind that only the samples with the highest sulfur areal and composite loading would be sufficient to achieve high energy densities on cell level [29]. Moreover, the average discharge potential lithium–sulfur batteries is about 40% lower (2.1 V vs. 3.7 V) than for lithium-ion batteries. Therefore, the areal capacity and current densities of sulfur cathodes have to be 75% higher than for lithium-ion ( $3.5 \text{ vs. } 2.0 \text{ mAh cm}^{-2}$ ) to achieve similar energy performances. This is the reason why a constant

current density in addition to the constant rate was tested. The current of  $1 \text{ mA cm}^{-2}$  corresponds to C/5 for a practical system with a theoretical capacity of  $5 \text{ mAh cm}^{-2}$ . At a typical sulfur utilization of  $1200 \text{ mAh g}^{-1}$  sulfur this equals the aspired areal capacity of  $3.5 \text{ mAh cm}^{-2}$ . It is important to note that high areal capacities require special electrode processing [5–7,26]. Unfortunately this can't be realized for the presented model system using a cathode with an open pore structure.

In addition, the amount of electrolyte would need to be less than  $4 \mu\text{l mg}_{\text{sulfur}}^{-1}$  and the lithium excess no larger than 100% to achieve energy densities exceeding state of the art lithium-ion battery cells. However, especially lowering the amount of electrolyte even further, when using lithium anodes, is non-trivial. We recently demonstrated that the main cell failure mechanism is that cells run dry. This is caused by the instability of the solvent molecules versus metallic lithium leading to their continuous decomposition [8]. However, this effect was only observed when a limited amount of electrolyte of  $12 \mu\text{l mg}_{\text{sulfur}}^{-1}$  was used. Beyond that, our group was able to demonstrate good results with high areal, composite loadings and sulfur utilizations with down to  $8 \mu\text{l mg}_{\text{sulfur}}^{-1}$  [30]. Accordingly, the minimum of  $20 \mu\text{l mg}_{\text{sulfur}}^{-1}$  identified by Zheng et al., that analyzed the influence of amount of sulfur and electrolyte at a constant rate, does not apply for our cell setup [23]. Nevertheless, even  $8 \mu\text{l mg}_{\text{sulfur}}^{-1}$  is still far away from assuming to only fill the porosity of the separator and the electrodes, as it is the case for lithium-ion batteries.

### 3.3. Influence of rate and amount of electrolyte

The cycle stability for the first 200 cycles of all samples is depicted in Fig. 3. It shows that the lowest degradation is observed for low sulfur content, high amount of electrolyte and a high C-rate (Fig. 3). The sulfur utilization decreases with increasing sulfur content in the cathode with no significant sulfur utilization for samples containing 80% sulfur. All cells show the typical dis-/charge voltage profile of lithium sulfur cells (see S4). In addition, the degradation for S20 and S40 is much higher at lower C-rates. At 2.5 C (S20-1 mA) a capacity of  $1190 \text{ mAh g}^{-1}$  sulfur is obtained in cycle 200. The same sample at 0.2 C falls below  $1190 \text{ mAh g}^{-1}$  sulfur after only 13 cycles. Interestingly, the slope of the discharge capacity at 0.2 C is very similar for 20 and 40%. Further, the capacity and degradation of the S60 samples (S60-C5 and S60-1 mA) is similar, as their C-rate only differs by a factor of 2. This suggests that a degradation mechanism exists, that correlates with time rather than the number of cycles.

For further prove, the sample S20-1 mA was stored fully charged at room temperature for 18 h after 500 and 41 h after 1000 cycles (Fig. 4). An irreversible capacity loss of 2.9% and 11.4%, respectively,

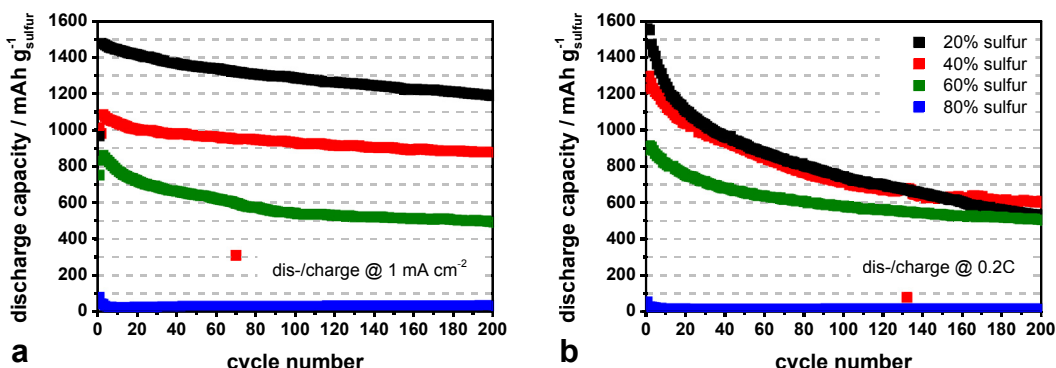
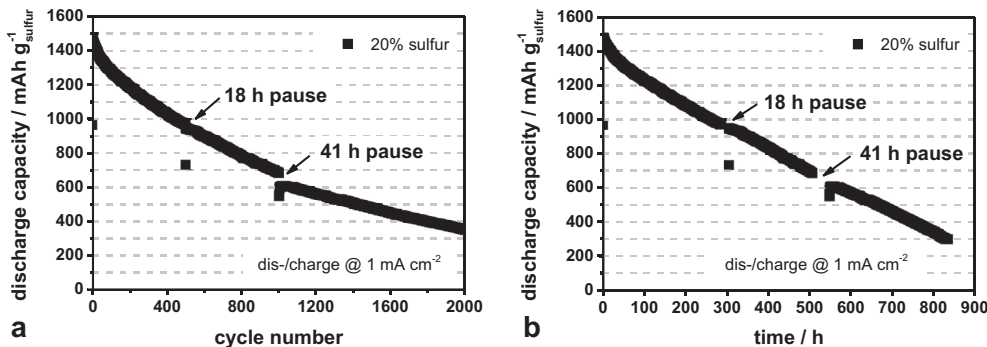


Fig. 3. First 200 cycles of all samples measured at  $1 \text{ mA cm}^{-2}$  (a) and C/5 (b).



**Fig. 4.** (a) Cycle performance for S20-1 mA up to 2000 cycles. Resting the sample fully charged at cycle 500 and 1000 resulted in an irreversible capacity loss of 2.9 and 11.4%, respectively. (b) Almost linear degradation is observed when the capacity is plotted versus the total cycle time rather than cycle number.

was observed after each pause. It appears to be an offset on top of the almost linear degradation of 0.06% and 0.08% per cycle, observed from cycle 100 to 500 and 502 to 1000.

The degradation at lower rates and after storage can be explained by the polysulfide dissolution in the electrolyte and their diffusion to as well as reaction with the anode. It was reported that high currents (short dis-/charge time) increase the coulombic efficiency (CE), since the diffusion of polysulfides to the anode is slower than the total electrochemical reaction time [31]. The CE is further improved by the use of lithium nitrate, which enhances SEI formation on the lithium anode [16,17]. As a result, the average coulombic efficiency is above 99% for all samples (see Table S1). Nevertheless, this does not necessarily mean that polysulfides shuttling is completely suppressed. Accordingly, we attribute the observed degradation for sample S20-1 mA to the reaction between polysulfides and the lithium metal anode, which results in a loss of active material. These parasitic self-discharge reactions are only slowed down but not completely suppressed. This indicates that the SEI formed using the lithium nitrate additive is not stable enough.

Our experiments show that higher currents and excess of electrolyte can give very good cycle stability. However, this may largely be caused simply by a lowered measurement time per cycle, which masks an underlying redox-reaction between reactive lithium and polysulfides (Fig. 4).

The samples containing 80% sulfur show almost no capacity. With respect to the areal loading and measured height, the estimated total “pore volume”, based on the tube interspaces of the VA-CNTs, is above  $5 \text{ cm}^3 \text{ g}^{-1}$  [5]. Consequently, a 10:1 loading with sulfur should be possible. However, our four to one ratio does not show complete sulfur incorporation into the VA-CNT network (S2).

This explains why no significant sulfur utilization is observed as most of the sulfur is not connected to the conductive carbon network. Due to the hydrophobic nature of carbon and sulfur strong adhesive forces occur, that lead to a very compact structure already at 60% sulfur content (S3). This highlights the necessity of specifically designed porous carbons [6,7] or hybrid structures [26] to realize functional cathodes with even higher composite loadings. Nevertheless, the model character of the presented system is sufficient in order to clearly demonstrate that only a balance of sulfur utilization and sufficient areal loading lead to practical electrodes (Fig. 5). Therefore, the order of samples is reversed when the capacity per gram electrode is plotted.

#### 4. Conclusions

In this paper, we used layer-transferred VA-CNT films as an almost ideal carbon material with aligned pores as a mechanically stable cathode host structure for the lithium sulfur battery. We demonstrated how an excess amount of electrolyte in combination with a high rate and low sulfur loading can lead to an increase in cycle life and capacity retention even in an arguably not ideal cathode system for realistic battery concepts. These parameters should also give a similarly significant performance increase to other host materials for the lithium–sulfur cathode. However, at the same time they prevent high energy densities on cell level, due to the dead weight of the electrolyte.

Our experiments showed that higher currents and excess of electrolyte can give very good cycle stability. Nonetheless, this may largely be caused simply by a lowered measurement time per cycle, which masks an underlying redox-reaction between reactive lithium and polysulfides.

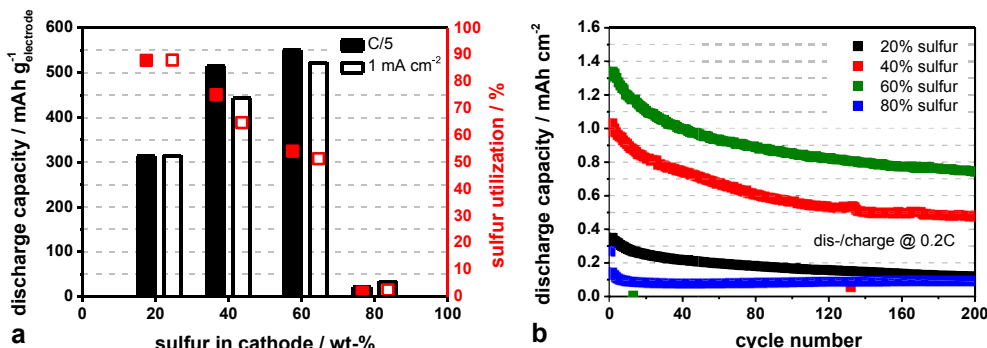


**Fig. 5.** (a) Cycle 3 discharge capacities per gram electrode versus sulfur utilization. Despite the continuous decrease in sulfur utilization (red: C/5 samples, black: 1 mA samples), the capacity per gram electrode increases from 20 to 60 wt.-% sulfur. (b) Areal discharge capacity for different samples at C/5. (For interpretation of the references to color in this figure legend, the reader is referred to the web version of this article.)

As a result, recently published data regarding sulfur cathode should be carefully interpreted. It is of utmost importance to question whether good sulfur utilization and cycle stability at low sulfur loading and high amount of electrolyte is really a result of improved material properties or should be mainly assigned to measurement parameters that are not applicable for realistic cell setups. Therefore, in future publications on lithium sulfur batteries, the amount of electrolyte and areal loading of sulfur used should be clearly stated.

## Acknowledgment

This research was financed by the Federal Ministry of Education and Research (BMBF, STROM: AlkaSuSi, FKZ: 03X4618A). We are grateful for the support.

## Appendix A. Supplementary data

Supplementary data related to this article can be found at <http://dx.doi.org/10.1016/j.jpowsour.2014.05.143>.

## References

- [1] R.D. Rauh, F. Shuker, J.J. Marston, Inorg. Nucl. Chem. 39 (1977) 1761, [http://dx.doi.org/10.1016/0022-1902\(77\)80198-X](http://dx.doi.org/10.1016/0022-1902(77)80198-X).
- [2] R.D. Rauh, K.M. Abraham, G.F. Pearson, J.K. Surprenant, S.B. Brummer, J. Electrochem. Soc. 126 (1979) 523, <http://dx.doi.org/10.1149/1.2129079>.
- [3] X. Ji, K. Lee, L. Nazar, Nat. Mater. 8 (2009) 500, <http://dx.doi.org/10.1038/NMAT2460>.
- [4] N. Jayaprakash, J. Shen, S.S. Moganty, A. Corona, L.A. Archer, Angew. Chem. Int. Ed. 50 (2011) 5904, <http://dx.doi.org/10.1002/anie.201100637>.
- [5] S. Dörfler, M. Hagen, H. Althues, J. Tübke, S. Kaskel, M.J. Hoffmann, Chem. Commun. 48 (2012) 4097, <http://dx.doi.org/10.1039/c2cc17925c>.
- [6] S. Thieme, J. Brückner, I. Bauer, M. Oschatz, L. Borchardt, H. Althues, S. Kaskel, J. Mater. Chem. A (2013), <http://dx.doi.org/10.1039/c3ta10641a>.
- [7] M. Oschatz, S. Thieme, L. Borchardt, M.R. Lohe, T. Biemelt, J. Brückner, H. Althues, S. Kaskel, Chem. Commun. 49 (2013) 5832, <http://dx.doi.org/10.1039/c3cc42841a>.
- [8] J. Brückner, S. Thieme, F. Böttger-Hiller, I. Bauer, H.T. Grossmann, P. Strubel, H. Althues, S. Spange, S. Kaskel, Adv. Funct. Mater. 24 (2014) 1284, <http://dx.doi.org/10.1002/adfm.201302169>.
- [9] X. Li, Y. Cao, W. Qi, L.V. Saraf, J. Xiao, Z. Nie, J. Mietek, J.-G. Zhang, B. Schwenzer, J. Liu, J. Mater. Chem. 21 (2011) 16603, <http://dx.doi.org/10.1039/c1jm12979a>.
- [10] Z. Wei Seh, W. Li, J.J. Cha, G. Zheng, Y. Yang, M.T. McDowell, Y. Cui, Nat. Commun. 4 (2013) 1331, <http://dx.doi.org/10.1038/ncomms2327>.
- [11] Y. Yang, G. Zheng, Y. Cui, Energy Environ. Sci. 6 (2013) 1552, <http://dx.doi.org/10.1039/c3ee0072a>.
- [12] S. Lu, Y. Cheng, X. Wu, J. Liu, Nano Lett. 13 (2013) 2485, <http://dx.doi.org/10.1021/nl400543y>.
- [13] M.-K. Song, Y. Zhang, E.J. Cairns, Nano Lett. 13 (2013) 5891, <http://dx.doi.org/10.1021/nl402793z>.
- [14] S. Moon, Y.H. Jung, W.K. Jung, D.S. Jung, J.W. Choi, D.K. Kim, Adv. Mater. 25 (2013) 6547, <http://dx.doi.org/10.1002/adma.201303166>.
- [15] X.-B. Cheng, J.-Q. Huang, H.-J. Peng, J.-Q. Nie, X.-Y. Liu, Q. Zhang, F. Wei, J. Power Sources 253 (2014) 263, <http://dx.doi.org/10.1016/j.jpowsour.2013.12.031>.
- [16] D. Aurbach, E. Pollak, R. Elazari, G. Salitra, C.S. Kelley, J. Affinito, J. Electrochem. Soc. 156 (2009) A694, <http://dx.doi.org/10.1149/1.3148721>.
- [17] Y.V. Mikhaylik, US 7354680 B2, 2008.
- [18] S.S. Zhang, Electrochim. Acta 70 (2012) 344, <http://dx.doi.org/10.1016/j.electacta.2012.03.081>.
- [19] C. Huang, J. Xiao, Y. Shao, J. Zheng, W.D. Bennett, D. Lu, S.V. Laxmikanth, M. Engelhard, L. Ji, J. Zhang, X. Li, G.L. Graff, J. Liu, Nat. Commun. 5 (2014) 3015, <http://dx.doi.org/10.1038/ncomms4015>.
- [20] W. Li, G. Zheng, Y. Yang, Z.W. Seh, N. Liu, Y. Cui, Proc. Natl. Acad. Sci. U. S. A. 110 (2013) 7148, <http://dx.doi.org/10.1073/pnas.1220992110>.
- [21] L.-X. Miao, W.-K. Wang, A.-B. Wang, K.-G. Yuan, Y.-S. Yang, J. Mater. Chem. A 1 (2013) 11659, <http://dx.doi.org/10.1039/C3TA12079A>.
- [22] M. Wang, W. Wang, A. Wang, K. Yuan, L. Miao, X. Zhang, Y. Huang, Z. Yu, J. Qiu, Chem. Commun. 49 (2013) 10263, <http://dx.doi.org/10.1039/C3CC45412F>.
- [23] J. Zheng, D. Lv, M. Gu, C. Wang, J.-G. Zhang, J. Liu, J. Xiao, J. Electrochem. Soc. 160 (2013) A2288, <http://dx.doi.org/10.1149/2.106311jes>.
- [24] F. Orsini, A. Du Pasquier, B. Beaudoin, J.M. Tarascon, M. Trentin, N. Langenhuizen, E. De Beer, P. Notten, J. Power Sources 76 (1998) 19, [http://dx.doi.org/10.1016/S0378-7753\(98\)00128-1](http://dx.doi.org/10.1016/S0378-7753(98)00128-1).
- [25] Y. Mikhaylik, I. Kovalev, R. Schock, K. Kumaresan, J. Xu, J. Affinito, ECS Trans. 25 (2010) 23, <http://dx.doi.org/10.1149/1.3414001>.
- [26] M. Hagen, S. Dörfler, H. Althues, J. Tübke, M.J. Hoffmann, S. Kaskel, K. Pinkwart, J. Power Sources 213 (2012) 239, <http://dx.doi.org/10.1016/j.jpowsour.2012.04.004>.
- [27] S. Dörfler, I. Felhösi, T. Marek, S. Thieme, H. Althues, L. Nyikos, S. Kaskel, J. Power Sources 227 (2013) 218, <http://dx.doi.org/10.1016/j.jpowsour.2012.11.068>.
- [28] K. Hata, D.N. Futaba, K. Mizuno, T. Namai, M. Yumura, S. Iijima, Science 306 (2004) 1362, <http://dx.doi.org/10.1126/science.1104962>.
- [29] M. Hagen, S. Dörfler, P. Fanz, T. Berger, R. Speck, J. Tübke, H. Althues, M.J. Hoffmann, C. Scherr, S. Kaskel, J. Power Sources 224 (2013) 260, <http://dx.doi.org/10.1016/j.jpowsour.2012.10.004>.
- [30] M. Oschatz, L. Borchardt, K. Pinkert, S. Thieme, M.R. Lohe, C. Hoffmann, M. Benusch, F.M. Wisser, C. Ziegler, L. Giebelter, M.H. Rümmeli, J. Eckert, A. Eychmüller, S. Kaskel, Adv. Energy Mat. 4 (2014) 1300645, <http://dx.doi.org/10.1002/aenm.201300645>.
- [31] Y.V. Mikhaylik, J.R. Akridge, J. Electrochem. Soc. 11 (2004) A1969, <http://dx.doi.org/10.1149/1.1806394>.